Intrusiveness of Power Device Condition Monitoring Methods

Introducing Figures of Merit for Condition Monitoring

Rizzo, Santi Agatino; Susinni, Giovanni; Iannuzzo, Francesco

Published in:
IEEE Industrial Electronics Magazine

DOI (link to publication from Publisher):
10.1109/MIE.2021.3066959

Publication date:
2022

Document Version
Accepted author manuscript, peer reviewed version

IEEE Industrial Electronics Magazine

Intrusiveness of Power Device Condition Monitoring Methods: Introducing Figures of Merit for Condition Monitoring

Santi Agatino Rizzo
Giovanni Susinni
Francesco Iannuzzo

Document Version:
Accepted author manuscript, peer reviewed version

Citation for published version:
S.A. Rizzo, G. Susinni and F. Iannuzzo, "Intrusiveness of Power Device Condition Monitoring Methods: Introducing Figures of Merit for Condition Monitoring," in IEEE Industrial Electronics Magazine, doi: 10.1109/MIE.2021.3066959.

Intrusiveness of Power Devices Condition Monitoring Methods

Power electronics is become pervasive in any electricity-based application, making power devices reliability an always more and more important topic. Maintenance operations are necessary to ensure the functioning of power electronics apparatuses [1]. Guessing the time for maintenance operation is challenging due to the related trade-off between maintenance cost and reliability improvement. Lifetime prediction techniques and condition monitoring methods (CMMs) are useful tools for determining the actual need [2].

Acoustic CMMs [3][4] detect any physical damages by using acoustic microscopes. The value and speed of the commutated current involve magnetic forces that are sources of acoustic emissions. These CMMs enable contactless monitoring thanks to an acoustic sensor usually placed close to the device package, but they need expensive and complex sensing circuits to correctly decode the emission and a shield against EMI and noise.

Several CMMs measure-estimate the junction temperature (Tj) since it plays a significant role, especially its continuous rapid variation, in power devices reliability.

Optical CMMs [4]-[6] exploit the dependence between temperature and photoemission. The use of an integrated photodiode placed, *a-priori*, by the devices manufactures or installed, *a-posteriori*, by the users enables contactless monitoring, but it is not being a mature technology [5]. CMMs based on the optical fibre present high resolution and fast response time but they are very expensive [6].

Physical CMMs [4][7] perform Tj measurement by contacting thermo-sensitive materials with the device surface. Various equipment has been used for the measurement: thermocouples, thermistors, scanning thermal probes, multiple contact or blanket coatings and so on. The setup also includes Wheatstone-bridge, opamps, filter to signal conditioning. The time response of the probe is the main limitation of thermal variations tracking. The need for contact is another limit that makes it useless in high voltage applications.

Electrical CMMs [4] exploit some temperature-related proprieties of the semiconductors. The temperature is esteemed by the measurement of electrical quantities: measurement of the voltage drop or the current that flows into the device can be used as valid temperature estimators.

Some electrical CMMs adopt thermal test chips (TTCs) [4][8] directly fabricated on the device surface: resistance temperature detector or diode. The former is usually an NTC thermistor. The voltage drop at its terminals varies with the resistance that depends on the temperature. Similarly, the latter exploits the change in the forward voltage to esteem the temperature variation. TTCs are exposed to degradation that may affect measurement accuracy.

The most widespread electrical CMMs are based on a thermo-sensitive electrical parameter (TSEP) [4], [9]-[18]. TSEP-CMMs use passive probes to measure electrical quantities at the device terminals, without direct access. These quantities are adopted for Tj estimation and, more in general, for analysing the state of health of the device. They are:

- *on-state voltage* - CMM mainly based on the conduction resistance dependence on Tj, they are based on low currents [10] or high pulsed currents [11],[12];
- *threshold voltage* - the CMM exploits the drop in the threshold voltage under increasing Tj [13];
- *saturation current* - CMM based on the current dependence from other quantities (mobility and so on) that depend on Tj [14];
- *gate-source (gate-emitter) voltage at turn-on/off* - the CMM uses the increment of the Miller plateau width with the temperature that can occur at turn-on or turn-off [15];
- *turn-on/off delay time* - the CMM considers, at turn-on, the increment with Tj of the delay between the device current rise starting and the related gate-source (gate-emitter) voltage rise starting, similarly, when the CMM focuses on turn-off, the delay between these falling quantities is considered [16];
- *peak gate current* - CMM exploiting the temperature-dependent behaviour of the internal gate resistance [17];

- *current and voltage switching speed* - CMM based on the dependence of the device switching waveforms rate on Tj [18].

Typically, the calibration setup of the CMMs based on the on-state voltage consists of a programmable current source and a temperature-controlled heat sink to set the initial temperature. Then, the temperature increase due to the current through the device is measured. Therefore, the voltage drop across the device is measured as a function of the temperature with a voltmeter, under known electrical conditions.

During the calibration of the threshold-voltage based CMMs, the gate and source (or emitter) terminals are shorted and a current source feeds the device while a voltmeter measures the threshold voltage. A similar setup is used for the CMMs exploiting the Miller plateau.

The measurement setup of the CMMs based on the saturation current consists of a voltage source connected between the gate and source (emitter) terminals and a DC voltage source connected between the drain (collector) and source (emitter) terminals of the device. The saturation current can be measured through the voltage drop on a shunt resistor.

The CMMs exploiting turn-on/off delay time require high bandwidth sensors and an advanced sampling circuit for temperature measurement. Furthermore, these methods usually require an external circuit to trigger a counter for the estimation of the turn-on and turn-off delay time.

The peak gate current based CMMs use the measurement of the peak voltage on the gate resistor during turn-on. A differential amplifier and a peak detector are adopted, then the data processed by an A/D converter are sent to a microcontroller for elaboration.

The measurement of the switching rate can be performed by a sensing circuit that detects the current and voltage transient dynamics. Hence, these CMMs require both high bandwidth sensors and the use of voltage and Rogowski coil probes.

Generally, TSEP-CMMs present a fast response time to the temperature transients and good accuracy, but their usage at the terminal limits the estimation granularity in the case of multi-die.

As far as the authors know there is not a study on the intrusiveness of the CMMs. In fact, many CMMs have been presented so far but only in a few cases, they discuss the intrusiveness of the proposed method. Very rarely these works compare the intrusiveness of the proposed CMM with others [19]. In the perspective of filling this gap, the work firstly proposes three intrusiveness criteria, then, it ranks and compares the CMMs in different ways according to these criteria. The comparison of different intrusiveness analyses has highlighted that the optic CMM adopting an integrated photodiode is usually the less intrusive.

Intrusiveness criteria

For a given criterion, a numerical mark is assigned to each CMM in the range from 1 (nonintrusive) to 10 (fully intrusive). Firstly, a mark equal to 1 has been assigned to the methods fully nonintrusive, then an incremental mark is assigned to the others by comparison with the ones already exanimated. Therefore, although the assignment of the mark is subjective, the rank of the CMMs according to an intrusiveness criterion is almost unbiased. Table 1 reports the legend(symbols) used in the following to indicate the CMMs and some information about their effectiveness.

Power device modification

The device modification criterion refers to alterations/changes in the power device structure due to a given CMM compared to the same device without employing any monitoring. The greater the modifications necessary to perform the measurement, the greater the CMM intrusiveness at the power device level: FOM_D is the intrusiveness index. In the following, the CMMs are ranked according to the device modification intrusiveness criterion, and the marks are assigned by adopting the procedure described before.

TSEPs CMMs present the lowest intrusiveness because the monitoring of the temperature can be carried out by exclusively measuring the electrical quantities at the device terminals. As evident, this approach does not require any modification of the device package or layout. Likewise, the acoustic methods (A) have also the lowest intrusiveness because the spectrometer is placed close to the device without any package modification. Hence, the FOM_D has been set equal to 1 for all these methods.

Table 1 – Condition monitoring methods: legend and effectiveness

Symbol	Method	Accuracy	Advantages	Drawbacks
A	acoustic [3][4]	↓	Contactless	Not mature Noise sensitive High cost
B	integrated photodiode sensor	↔	Contactless	Not mature
C	postdated photodiode sensor [5]	↔		
D	optical fibre [6]	↑	High sensitivity High accuracy	High cost
E	physical [7]	↔	Good linearity Good sensitivity	Poor response time Obsolete
F	TTC NTC thermistor [8]	↓	Good linearity	Ageing sensitive
G	TTC diode [8]	↔	Good sensitivity	Poor linearity
H	TSEP on-state-voltage @ low-current [10]	↑	High sensitivity High linearity Easy calibration	High cost
I	TSEP on-state-voltage @ high-current [11][12]	↓	High linearity	High cost Ageing sensitive Load current dependence
J	TSEP threshold voltage [13]	↔	Good sensitivity Good linearity	Unplug the DUT
K	TSEP saturation current [14]	↔	High sensitivity	Poor linearity
L	TSEP gate-source (gate-emitter) voltage at turn-on/off [15]	↔	High linearity	High-cost sensing Inaccurate measurement
M	TSEP turn-on/off delay time [16]	↓	High linearity Low parameter-dependent	Ageing sensitive High-cost sensing
N	TSEP peak gate current [17]	↔	Good linearity Easy-implement	Ageing sensitive High-cost sensing
O	TSEP current and voltage switching speed [18]	↔	Good sensitivity Good linearity	High cost Gate resistance dependence

The optical CMM adopting the optical fibre (D) is a little more intrusive since it requires to drill two small holes in the packaging to insert the optical fibre wires close to the device chip: FOM_D=2.

The intrusiveness of the optical CMMs based on photodiode sensors inside the package should be distinguished in two different scenarios: integrated (i.e. *a priori*) photodiode (B) and postdate photodiode, that is placed *a posteriori* (C). In the first scenario, the overall layout can be optimized by the manufacturer so that the device performs well meanwhile the modification could be very limited. On the other hand, the device modifications are more than a simple hole on the package: FOM_D=4. In the second scenario, the device packaging has to be opened and the photodiode placed by a user. Hence, the postdated approach entails higher intrusiveness compared to the integrated one: FOM_D=5.

The use of TTCs, such as the thermistors (F) and integrated diodes (G), that are usually fabricated on the surface of the die, involves that the internal layout and the pins of the power module have to be redesigned from the original ones: FOM_D=8 (F) and FOM_D=7 (G). The different value is due to the grater cumbersome of the former.

Finally, the CMM using the thermocouple (E) is the most intrusive due to the need to open the device packaging and usually to modify the layout to effectively place the thermocouple. Moreover, the device packaging must be drilled to place the BNC cables for the measurements: FOM_D=9.

Figure 1 summarizes the values of FOM_D.

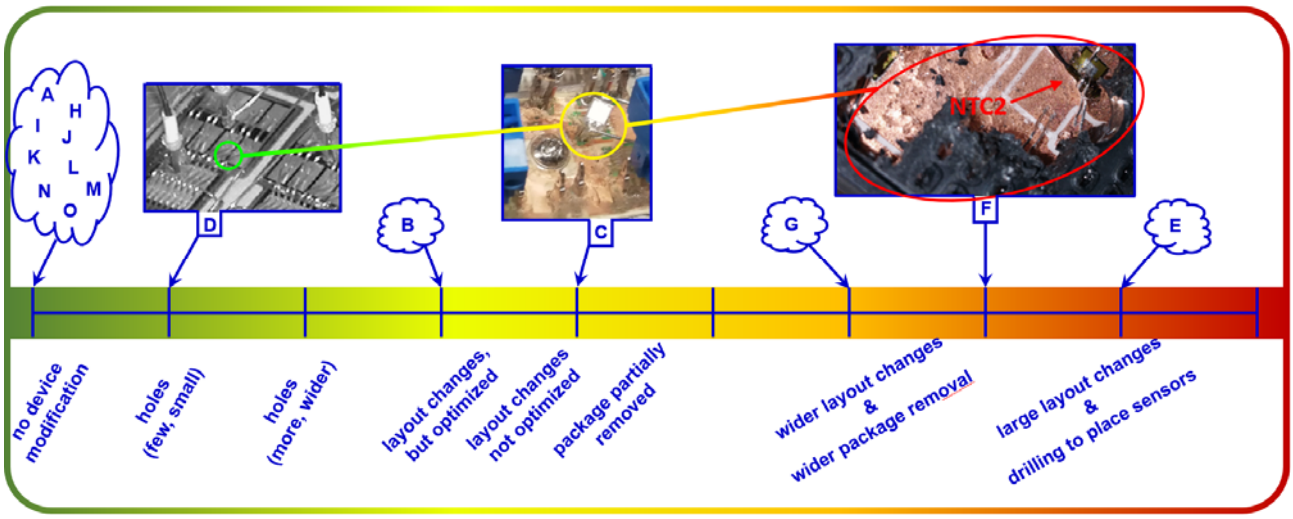

Figure 1. FOM_D assigned to the CMMs. Embedded pictures respectively from [6],[5],[12].

Modification of power conversion system operation

The conversion system operation criterion refers to the impact of a CMM on the normal working operations of a power converter: change in the operating conditions, forced shut-down, converter unplugging and so on. Moreover, the electrical probes have several limitations in their use such as limited bandwidth, intrinsic parasitic capacitances, and also, they cannot always be used for high voltage operations. Therefore, the use of the voltage or current probes could involve a slight perturbation.

In the following, each CMM has been analysed to fully understand the intrusiveness level. The CMMs are ranked according to their intrusiveness level and incremental marks are assigned by adopting the procedure described before: FOM_C is the intrusiveness index.

The lowest value of FOM_C is assigned in case of online monitoring without any physical contact between the conversion system and the measurement system (e.g. without probes or wires). Therefore, all the optical CMMs present the lowest intrusiveness since they are based on the measurement of the light brightness or the measurement of the emissivity change. Also, the acoustic method (A) does not affect the converter operations. Hence, all these CMMs have $FOM_C=1$.

The physical methods (E) and the TTCs (F and G), have a slightly higher level of intrusiveness since a voltage probe is used on the power module external connectors. Therefore, according to some previous considerations, the sensing equipment may introduce a few disturbances: $FOM_C=2$.

The TSEPs turn-on/off delay time (M) and peak gate current (N) CMMs can carry out the Tj monitoring during online working operations, but the use of at least two probes is mandatory: $FOM_C=3$.

The on-state voltage at high current (I) also allows online Tj monitoring, but at cost of a high current injected into the device. Notwithstanding the ability to monitor the Tj during online operations, the pulsed current injected into the device must have a time width of hundreds of microseconds. Consequentially, the converter operations change for a short time from the typical functionalities each time the monitoring is performed. In this case, the FOM_C has been set equal to 6 due to the high alteration in the converter system, which is strongly greater than the previous methods.

The CMMs based on the on-state voltage under low-level injection (H), the saturation current (K) and the gate-source (gate-emitter) voltage at turn-on/off (L) often cannot be used online except in limited cases and need very complex circuits to mitigate their impact on the converter [9]: $FOM_C=9$.

The threshold voltage (J) and the voltage-current switching speed (O) are TSEPs that involve CMMs with the highest level of intrusiveness. These methods need to unplug the converter to perform the Tj measurement: $FOM_C=10$.

Figure 2 summarizes the values of FOM_C for each CMM.

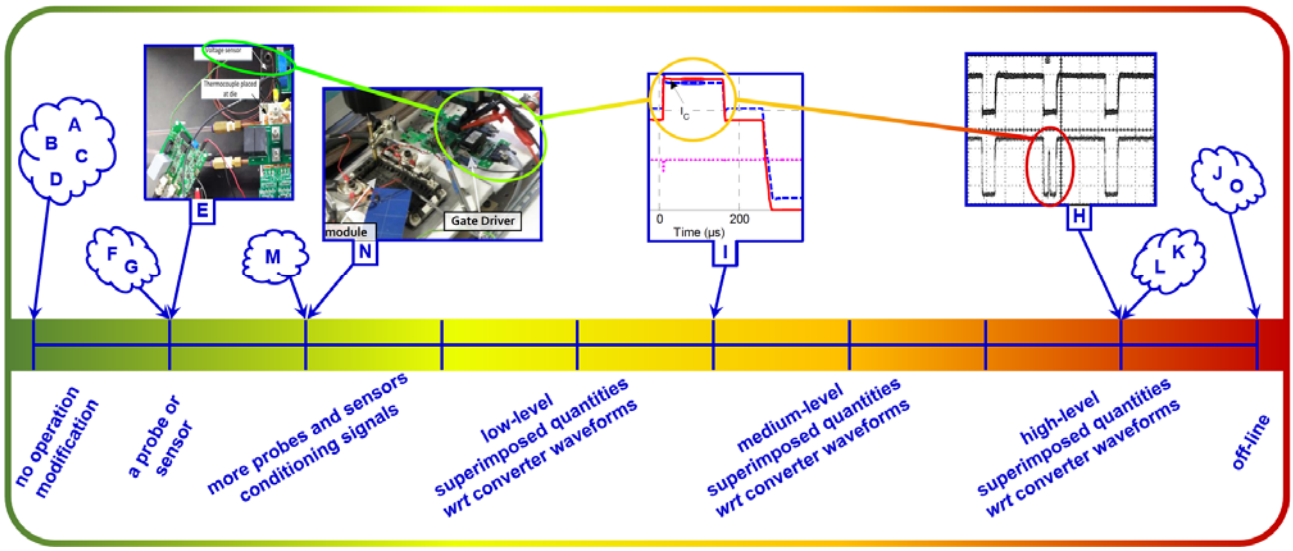

Figure 2. FOM$_C$ assigned to the CMMs. Embedded pictures respectively from [7],[17],[11],[14].

System modification

The system modification criterion highlights the level of changes in the system components (power converters, funs, loads, power supplies and so on) as well as their interconnections, that can also be *ad hoc* for a specific application. This criterion also accounts for the use of cumbersome tools for data acquisition, the need to open the chassis protection of the system, whereas the auxiliary circuitry may be bulky respect the application and so on. Once again, the CMMs have been analysed to highlight their intrusiveness level: FOM$_S$ is the intrusiveness index.

The measurement of Tj using an integrated photodiode (B) requires only the measurement of the voltage drop on the resistor. Hence, there is not any modification in the system, neither the addition of auxiliary electrical circuits compared to the scenario without monitoring: FOM$_S$=1. The most recent CMM adopting a postdated photodiode (C) involve a little higher intrusiveness since it usually needs a small board for signal conditioning (R-C circuit) [5]. Similarly, TTCs based methods (F-G) require the measurement of the voltage variation by using a voltmeter sensing circuit. Therefore, the intrusiveness level in the real system is lightly higher: FOM$_S$=2.

The thermocouples (E) lead to a further slight increment in the intrusiveness level because an auxiliary circuit (Wheatstone-bridge, opamps and so on) detecting the resistance variation with the temperature is usually employed. The turn-on/off delay time (M) CMM requires a sensing circuit

(opamps, FPGA and so on) that may be integrated into the gate driver, otherwise, the auxiliary sensing circuits are placed close to the converter system. The peak gate current (N) method uses two voltages probes and a detecting circuit (instrumentational amplifier, filter and so on) to measure the voltage variation on the gate resistance. Thus, for all of them: FOM_S=3.

The on-state voltage at a low current injection (H) method also requires a sensing circuit (opamps, filter and so on) to measure the voltage variation at turn on-off but, in addition, it needs an active clamping circuit for low voltage values, thus involving greater intrusiveness: FOM_S=4.

The threshold voltage (J) and gate-source (gate-emitter) voltage at turn-on/off (L) CMMs require a low current generator for the calibration step. For example, considering an IGBT device, the gate and the collector terminals are shorted and then, the gate-emitter voltage drop is measured through a voltmeter. Hence, the gate driver has to be modified to perform the measurement. Similar reasoning can be carried out in case of the voltage-current switching speed (O) TSEP-CMM. Therefore, FOM_S=5.

The on-state voltage at high injected current (I) CMM requires a high DC pulsed current source that feeds the device by using several switches and a voltmeter for the device voltage drop measurement. This CMM is low accurate and, consequently, sophisticated and cumbersome sensing circuits are used. Therefore, it shows a higher level of intrusiveness in the overall system: FOM_S=7. Similarly, the saturation current (K) CMM requires a DC source and a switch to injecting a current pulse (hundreds of microseconds). Furthermore, an auxiliary circuit is necessary to detect the saturation current, making the system intrusiveness comparable with I.

The CMM based on the acoustic (A) emission requires an advanced sensing circuit and a bulky data acquisition station (a server, several A/D converters, a dedicated power supply system) sometimes not easy to integrate with the pre-existing application. This larger volume is then due to the circuitry required by the acoustic spectrometer adopted by the methods, which also needs the chassis removal to place the spectrometer close to the power device. Similar considerations are valid for CMM adopting optical fibre (D). Thus, they are the most intrusive: FOM_S=8.

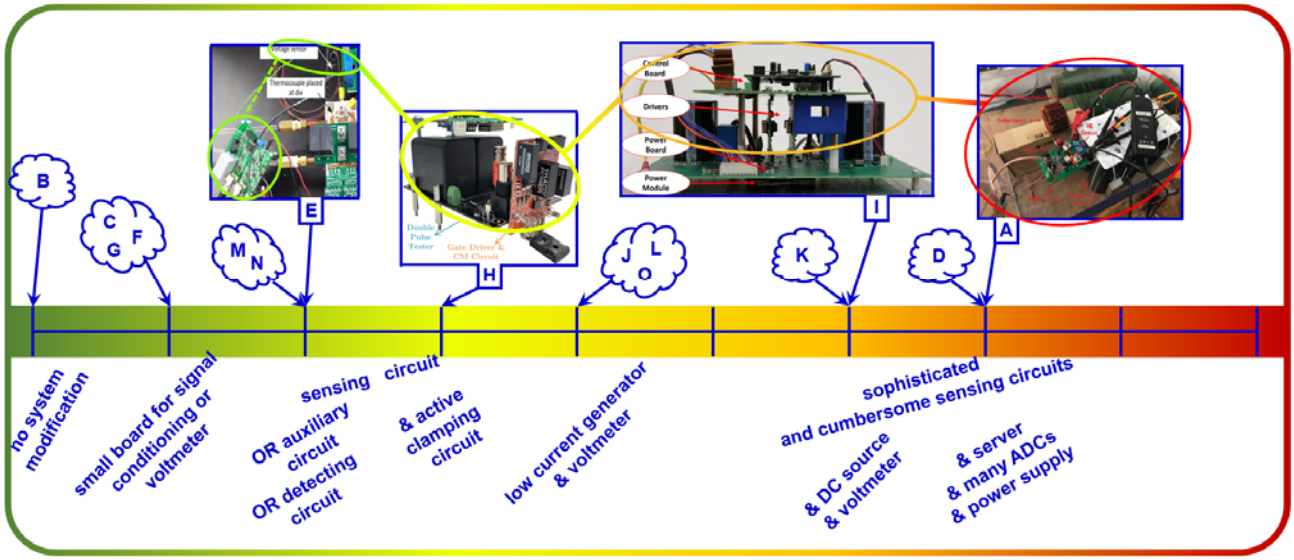

Figure 3. FOMs assigned to the CMM. Embedded pictures respectively from [7],[10],[12],[3].

Figure 3 summarizes the FOMs value assigned to each CMM.

Generalized comparison method of the CMMs intrusiveness

The adoption of a unique FOM representing the general level of intrusiveness of a CMM is highly desired. The product of all the previous intrusiveness indices is the simplest way to obtain an overall intrusiveness FOM, named IFOM:

$$IFOM(m) = FOM_D(m) * FOM_C(m) * FOM_S(m)$$
$$IFOM_{norm}(m) = 10\frac{IFOM(m)}{max(IFOM)} \qquad m = A, B, \dots, O \qquad (1)$$

Fig.4 reports the value of IFOM normalized, in]0, 10], $IFOM_{norm}$, thus highlighting that the saturation current (K) TSEP leads to the most invasive CMM. It is worth remembering that the monitor of Tj can be carried out only by switching off the power converter. Moreover, it requires the use of a DC source and a switch that controls the injection of a current pulse width of hundreds of microseconds. Also, Tj monitoring can be estimated by using an auxiliary circuit that must be able to detect accurately the saturation current of the device. In this perspective, the high values both of FOM_C and FOM_S lead to an increase in the overall intrusiveness. The CMM based on integrated (i.e. *a priori*) photodiode (B) is the less intrusive one since there is only a low impact at device level due to the need for layout modification.

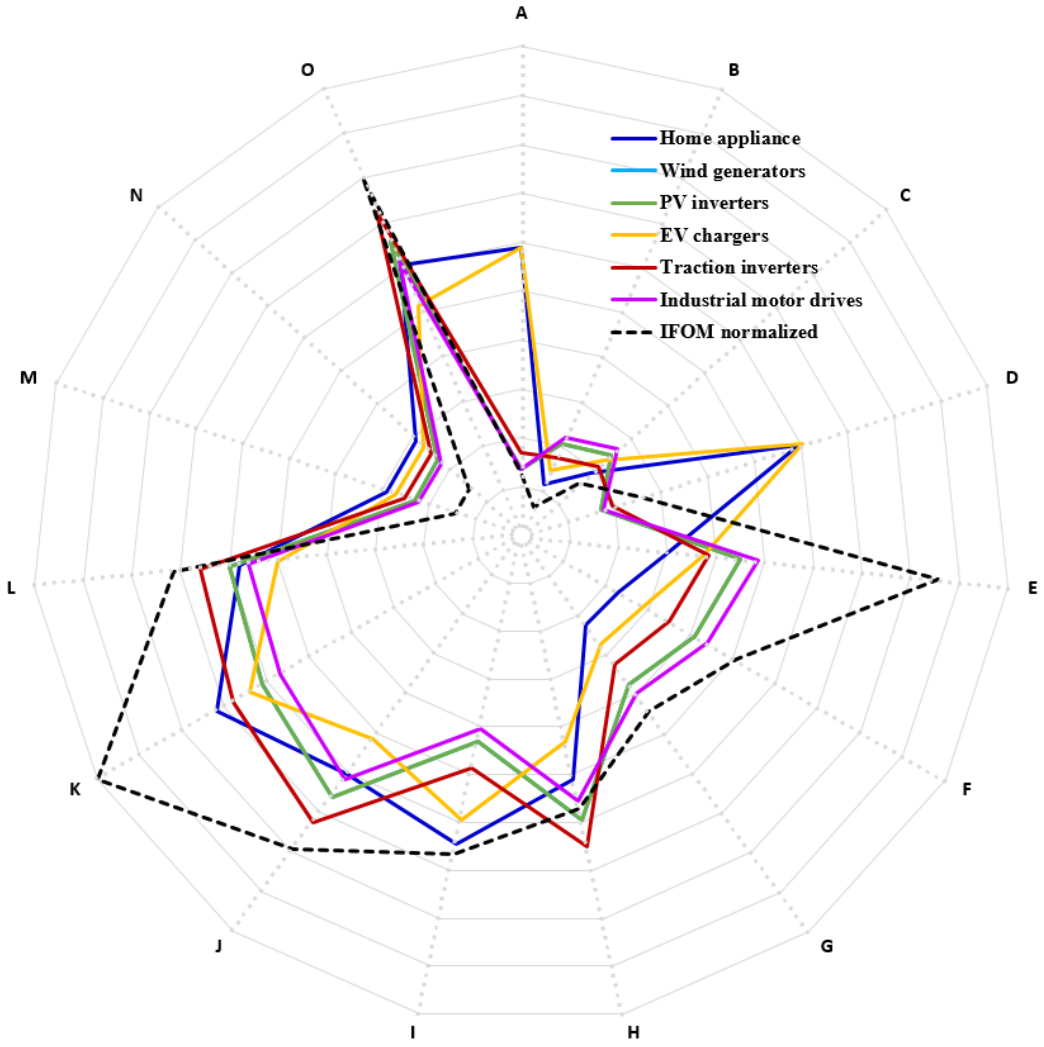

Application	w_1	w_2	w_3
Home appliance	0.05	0.25	0.70
Wind generators	0.35	0.60	0.05
PV generators	0.35	0.60	0.05
EV chargers	0.15	0.15	0.70
Traction inverters	0.25	0.65	0.10
Industrial motor drives	0.40	0.55	0.05

Figure 4. Normalized IFOM and application-based FOM (in different applications) assigned to the CMMs

The CMMs exploiting the integrated photodiode (B) are the less intrusive ones. The use of an integrated photodiode does not introduce system modification and the Tj can be estimated during the online converter operations. The greatest impact is due to the need for some layout modifications. Finally, an application-related invasiveness FOM has been defined. More specifically, A FOM accounting for all the intrusiveness criteria and their importance in specific applications.

For a given CMM, m, and a specific application, a, the related FOM, $f_a(m)$, is computed as follows:

$$f_a(m) = w_{a,1} \cdot FOM_D(m) + w_{a,2} \cdot FOM_C(m) + w_{a,3} \cdot FOM_S(m)$$
$$w_{a,1} + w_{a,2} + w_{a,3} = 1 \quad (2)$$

where $w_{a,1}$, $w_{a,2}$, and $w_{a,3}$ are weights proportional to the importance of each intrusiveness criterion in the specific application. More in general, f_a is a normalized FOM and the weights are the normalizing factors.

Fig.5 enables to better understand the different meaning of the three proposed figure of merits, and how a user must set the weights in equation (2). An important aspect is that, for a given CMM, the values of FOM_D, FOM_C and FOM_S are independent among them and independent from the application. Instead, the weights must be assigned by the user according to their different importance in the specific application. For example, in a dusty or moist environment or in an application where atmospheric agents could damage the device, the device intrusiveness criterion is important: $w_{a,1}$ must be high. In applications where electric contacts with the converter or the converter shut-down must be avoided, the converter operation intrusiveness criterion is important: $w_{a,2}$ must be high. In applications requiring high power density or, more in general, where the weight and encumbrance of the conversion system must be minimized, the system intrusiveness criterion is important: $w_{a,3}$ must be high.

Fig.4 also reports some weights (on the right) that could be assigned in different applications and the related values of the application-based-FOM (on the left). For example, in a wind farm, the on-line monitoring is fundamental. Therefore, in such an application, $w_{a,2}$ should be set higher than the others, although gaps in the device package should be avoided, especially in some applications, e.g. offshore wind farms, where the high humidity could damage the device. The size of the CM system should be considered in micro-wind-generators but, in this application, CM is less important compared with large power plants. The weights in Fig.4 ('Wind generators') account for these considerations and the importance of CM in the different applications. All other weights in Fig.4 are assigned by using similar reasoning, but for a specific application, the user must set the weights by accounting for the trade-off among the importance of the three intrusiveness criteria. This involves a subjective answer, i.e. weights assignment, to the questions on the right side of Fig.5.

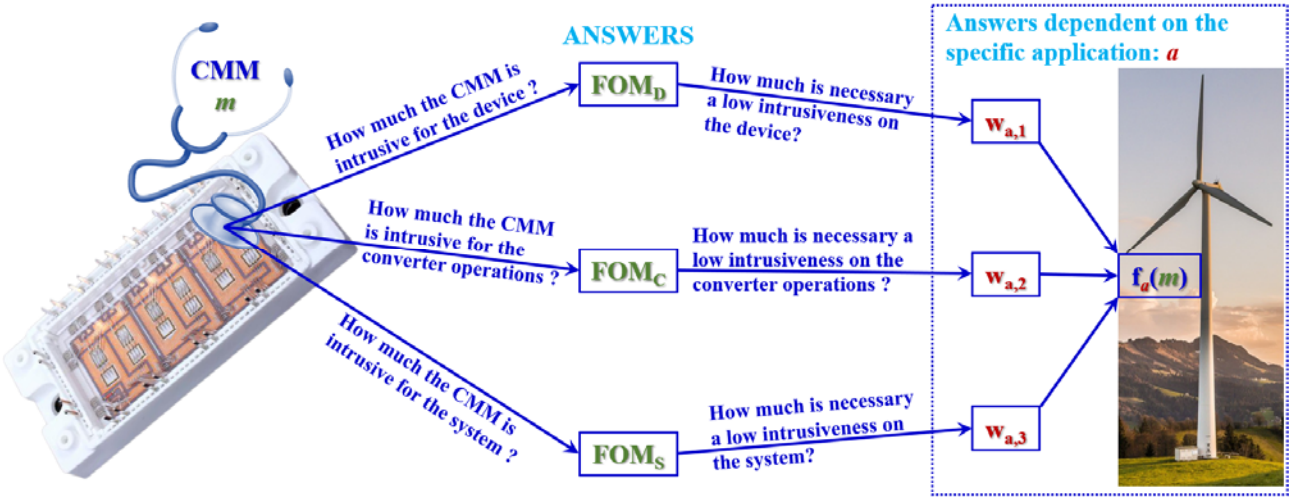

Figure 5. Meaning of the proposed figure of merits and of the weights in equation (2).

Finally, since the weights change as the application changes, there is not a CMM whose f_a is always better than the others. Considering the increasing application fields of Power Electronics as well as the deeper use in traditional sectors, it is necessary to develop CMMs tailored for the specific application. To this aim, the reported analyses and the proposed comparison approach have the merit of point to the potential candidates to be properly customized.

A good feature of these FOMs is to provide a single value which is useful to compare the CMMs since it accounts for the three intrusiveness criteria. On the other hands, they may suffer from the biased marks assigned by the authors according to each criterion.

Considering that:

- the target of this work is to provide a tool for intrusiveness comparison;
- the ranking of CMMs according to an intrusiveness criterion is almost unbiased;

the Pareto optimality [20] reasoning has been proposed to effectively perform the comparison.

According to Pareto optimality, Figure 6 reports a simple visual inspection that concurrently compares the CMMs in terms of the three intrusiveness criteria. More specifically, each method has been represented by a circle in the figure. The couple of values FOM_D-FOM_S represent the centre of the circle, while the circle radius is set about proportional to FOM_C. Moving from the left to the right, the CMMs are ordered for worsening FOM_D. Similarly, they are ordered for worsening FOM_S moving from the bottom to the upside. Therefore, whether the circle associated to a CMM is placed below

another one and it is also on the left of the latter, the former is better in terms of intrusiveness provided that it presents a circle size equal or lower than the latter.

To formalize the comparison, some concepts are borrowed from the Pareto efficiency analysis. A CMM, Ψ, is said optimum, according to the Pareto optimality when [20]:

$$\begin{cases} \nexists\, m \in \{A, B, \dots Q\} : \\ FOM_D(\Psi) \geq FOM_D(m) \\ FOM_C(\Psi) \geq FOM_C(m) \\ FOM_S(\Psi) \geq FOM_S(m) \\ relation > is\ true\ for\ at\ least\ one \end{cases} \tag{3}$$

In other words, a CMM Ψ is said optimum when there is not any CMM better of it. In Figure 6, the green circles represent all the optimum CMMs, that is the methods satisfying (3), while the red circles represent the others, that is the CMMs for which exist another CMM with lower intrusiveness from all point of views (criteria).

Figure 6 reminds that the acoustic CMMs (A) and all TSEP-CMMs (H-O) have the same FOM_D. Among these, H, J, L, O, I and K are worse than M (which is equivalent to N) from both the other criteria. Consequently, they are not optima (red circles). Acoustic CMMs (A) present worse FOM_S than O but better FOM_C (smaller circles), the A, M, N are optimum in terms of intrusiveness (green circles).

The circle related to the optical fibre (D) CMM presents the same radius of the one representing A, but the latter has lower FOM_D, then D is not optimum (red circle).

The remaining CMMs such as the ones based on the external photodiode (C), the TTCs (G-F) and the Thermocouple (E) are located in the upper-right-side of the integrated photodiode CMM (B). Moreover, none of them presents a lower FOM_C (i.e. lower radius) than B. Then, they are not optima (red circles). The circle related to method B is on the right of A, M, N, i.e. B is worse of them in terms of device intrusiveness, but it presents the lowest intrusiveness in the conversion system (FOM_S). Therefore, B is optimum (green circle).

It is worth to notice, that the adoption of CMM ranking, instead of the mark, has enabled to exploit Pareto optimality to compare the various CMMs effectively also thanks to the intuitive representation

method proposed in Fig.6. In fact, by analysing the figure differently, it is immediately apparent that there is not a CMM better than B, thus B is an optimal solution. It is concurrently evident that all the CMMs located on its upper-right side (C, E, F, G) are worse than B considering that there is not any circle smaller than those assigned to B. In other terms, there is not an intrusiveness criterion for which the CMMs C, E, F and G are better than B, *vice versa* there is at least a criterion for which B is better of them. At the same time, it is concurrently evident that all the CMMs located on the left (A, D, H-O) of B are not worse of it, thus they have to be analysed among them only. From their analysis it is immediately apparent that there is not a CMM better than M and N, thus M and N are the optimal solutions. It is concurrently evident that all the CMMs located above them and with a greater radius (H-L, O) are worse than M and N. In other terms, there is not an intrusiveness criterion for which the CMMs H-L, O are better than M and N, *vice versa* there is at least a criterion for which M and N are better of them. At the same time, it is concurrently evident (lower radius) that A and D are not worse of M and N, thus they have to be analysed among them only. From the comparison of A and D, it is obvious that the former is better than the latter since in it on the left. and they are located at the same height and present the same radius.

By summing up, the acoustic methods (A), the ones based on an integrated photodiode sensor (B), the CMMs based on the TSEP turn-on/off delay time (M) and on the TSEP peak gate current (N) are the optimum CMMs. This implies that, whatever the weights on equation (2), i.e. in any application, the less intrusive CMM is one (or more) among A, B, M and N, while the less intrusive CMM never could be one among C-L and O. Consequently, the main outcome is that, regardless the application, the user must choose only among A, B, M and N when the selection criterion is based only on the intrusiveness.

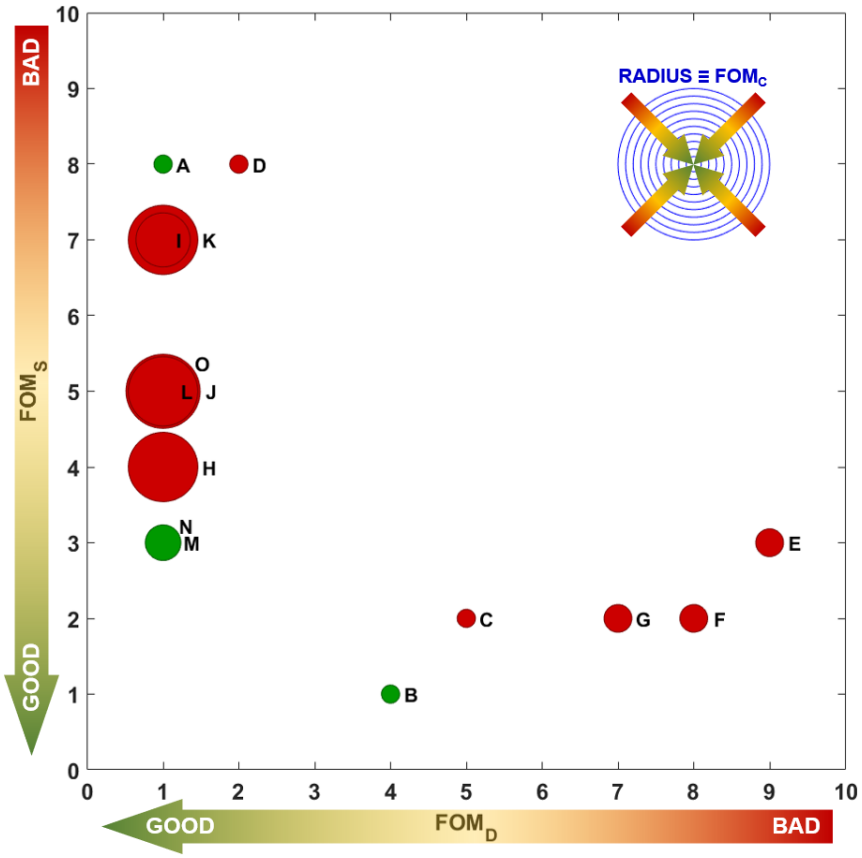

Figure 6. FOM_D-FOM_S represent the circle centre, the circle radius is proportional to FOM_C

Conclusion

The intrusiveness of the CMMs has been investigated and three intrusiveness criteria have been considered at the device level, converter operation level, and conversion system level to rank the CMMs. Pareto optimality has been adopted to concurrently compare them effectively also thanks to the proposed intuitive representation method. The comparison revealed that the CMMs adopting acoustic sensors or integrated photodiode or two TSEPs (turn-on/off delay time or peak gate current) are the best ones in terms of intrusiveness. More specifically, the main outcome of the intrusiveness analysis and comparison is that, regardless of the application, the user must choose only among them when the selection criterion is based only on the intrusiveness. On the other hand, other aspects, e.g. effectiveness and cost, are important. The comparison of the CMMs in terms of effectiveness is a critical aspect that deserves to be investigated in future works. Finally, the CMM that adopt integrated photodiode is the least intrusive according to the overall FOM, although this technology is currently not enough mature. A crucial aspect that emerged from the analysis is the need for CMMs customized

for specific application typology. Therefore, given the always wider and wider application fields of Power Electronics, the future research on condition monitoring of power device must be more than ever application-oriented.

References

[1] S. Peyghami et al. "A Guideline for Reliability Prediction in Power Electronic Converters," Transactions on Power Electronics, vol.35, no.10, pp.10958-10968, 2020.

[2] A. Hanif et al. "A Comprehensive Review Toward the State-of-the-Art in Failure and Lifetime Predictions of Power Electronic Devices," Transactions on Power Electronics, vol.34, no.5, pp.4729-4746, 2019.

[3] M. Li et al. "Acoustic Emission-Based Experimental Analysis of Mechanical Stress Wave in IGBT Device," IEEE Sensors Journal, vol.20, no.11, pp.6064-6074, 2020.

[4] S. Yang, et al. "Condition Monitoring for Device Reliability in Power Electronic Converters: A Review," Transactions on Power Electronics, vol.25, no.11, pp.2734-2752, 2010.

[5] G. Susinni et al. “A non-invasive SiC MOSFET Junction temperature estimation method based on the transient light Emission from the intrinsic body diode”, Microelectronics Reliability, vol.114, no.113845, 2020.

[6] Z. Khatir et al. "Real-time computation of thermal constraints in multichip power electronic devices," Transactions on Components and Packaging Technologies, vol.27, no.2, pp.337-344, 2004.

[7] M.H.M. Sathik et al. "Online junction temperature for off-the-shelf power converters," APEC, pp.2769-2774, 2018.

[8] A. Claassen et al. “Comparison of diodes and resistors for measuring chip temperature during thermal characterization of electronic packages using thermal test chips.” IEEE Semiconductor Thermal Measurement and Management Symposium, pp.198-209,1997.

[9] Y. Avenas et al. "Temperature Measurement of Power Semiconductor Devices by Thermo-Sensitive Electrical Parameters—A Review," Transactions on Power Electronics, vol.27, no.6, pp.3081-3092, 2012.

[10] E. Ugur et al. "A New Complete Condition Monitoring Method for SiC Power MOSFETs," Transactions on Industrial Electronics, vol.68, no.2, pp.1654-1664, 2021.

[11] L. Dupont et al. "Evaluation of thermo-sensitive electrical parameters based on the forward voltage for on-line chip temperature measurements of IGBT devices," IEEE ECCE, pp.4028-4035, 2014.

[12] F. Stella et al. "Online Junction Temperature Estimation of SiC Power MOSFETs Through On-State Voltage Mapping," Transactions on Industry Applications, vol.54, no.4, pp.3453-3462, 2018.

[13] H. Chen et al. "On-line monitoring of the MOSFET device junction temperature by computation of the threshold voltage", IET Int. Conf. Power Electron. Mach. Drives, pp.440–444, 2006.

[14] D. Bergogne et al. "An estimation method of the channel temperature of power MOS devices," IEEE Annual Power Electronics Specialists Conference, vol.3, pp.1594-1599, 2000.

[15] Y. Avenas et al. "Comparison of junction temperature evaluations in a power IGBTs module using an IR camera and three thermo-sensitive electrical parameters", APEC, 2012.

[16] M. Du et al. "Estimating Junction Temperature of SiC MOSFET Using Its Drain Current During Turn-On Transient," Transactions on Electron Devices, vol.67, pp.1911-1918, 2020.

[17] N. Baker et al. "IR Camera Validation of IGBT Junction Temperature Measurement via Peak Gate Current," Transactions on Power Electronics, vol.32, no.4, pp.3099-3111, 2017.

[18] A. Bryant et al. "Investigation into IGBT dV/dt during turn-off and its temperature dependence," Transactions Power Electronics, vol.26, pp.3019–3031, 2011.

[19] G. Susinni, S. A. Rizzo, and F. Iannuzzo, "Two Decades of Condition Monitoring Methods for Power Devices," Electronics, vol. 10, no. 6, p. 683, Mar. 2021.

[20] E. Zitzler et al. "Performance assessment of multiobjective optimizers: an analysis and review," Transactions on Evolutionary Computation, vol.7, no.2, pp.117-132, 2003.